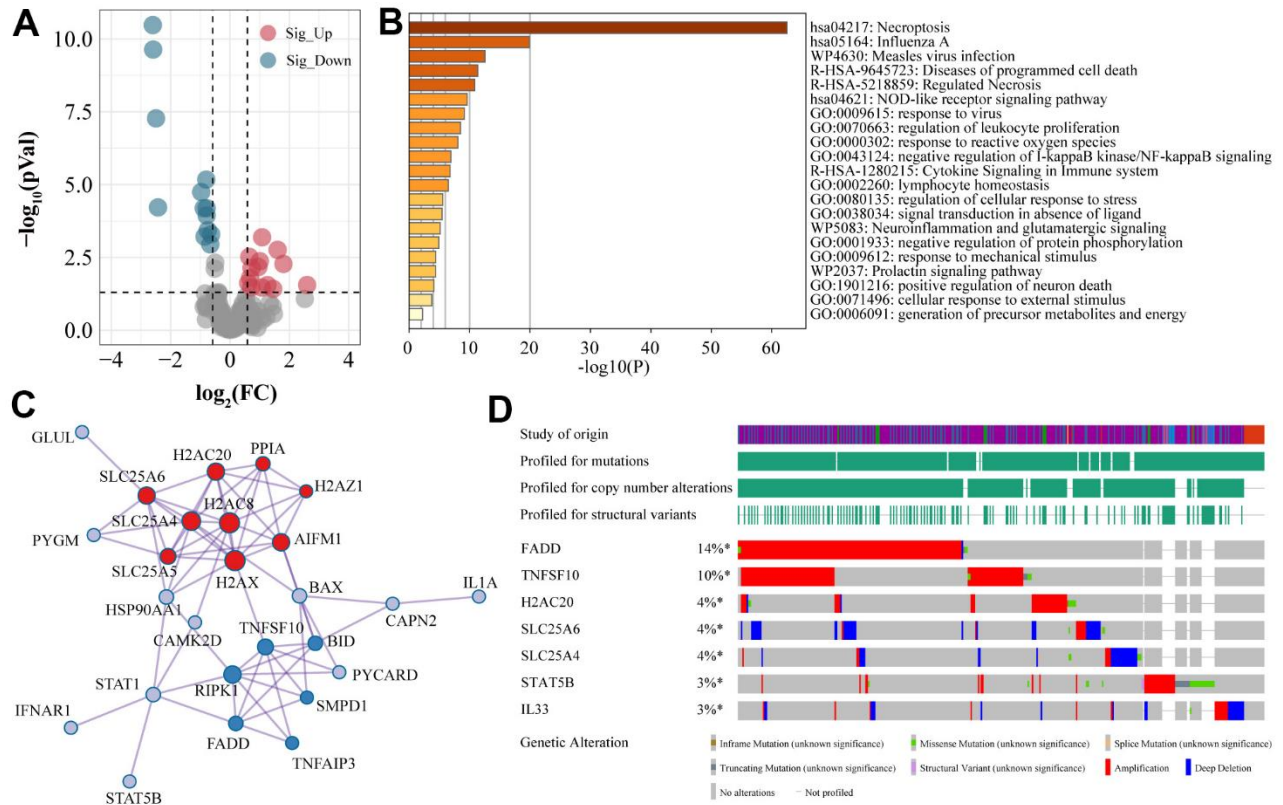
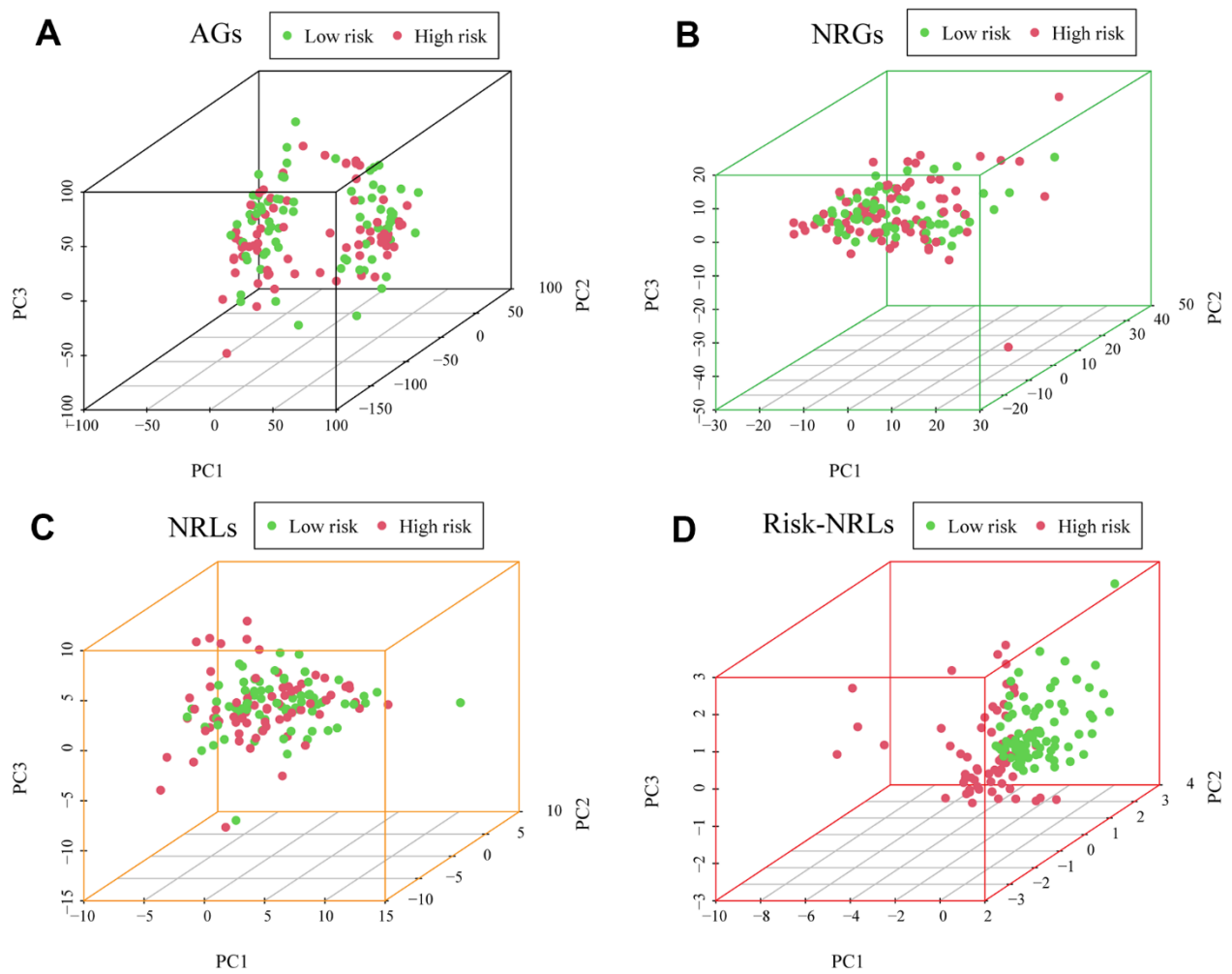


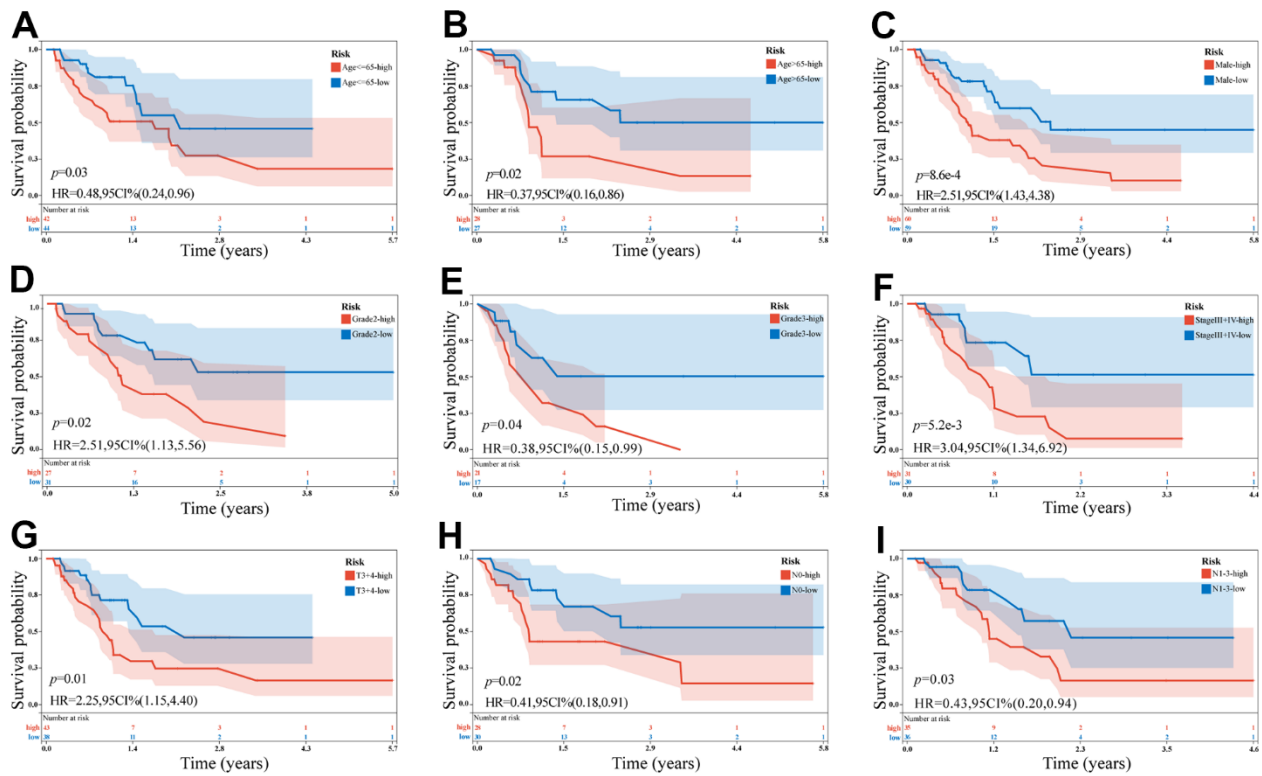
SUPPLEMENTARY FIGURES



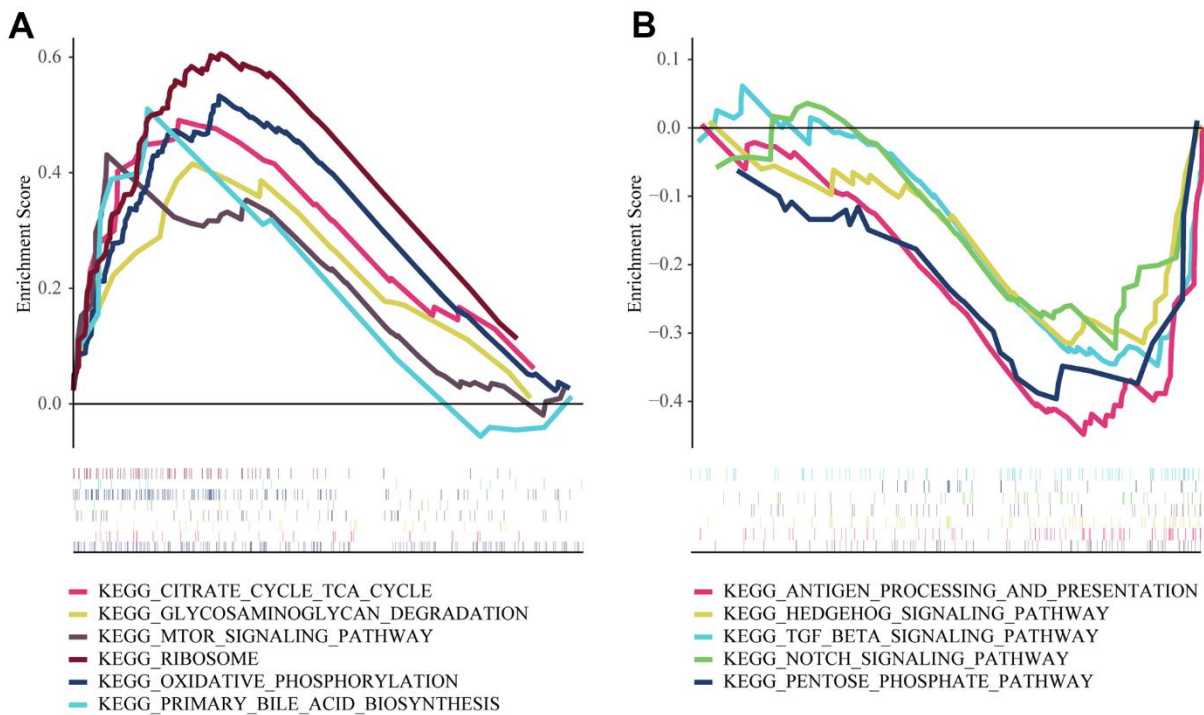
Supplementary Figure 1. The differentially expressed, interaction, and mutation analysis of NRGs. (A) The volcano plot of the significantly different expression of NRGs in ESCA and adjacent tissues. **(B)** KEGG enrichment analysis of differentially expressed NRGs. **(C)** A PPI network showed interactions of NRGs. **(D)** A total of seven NRGs have a mutation rate of $\geq 3\%$.



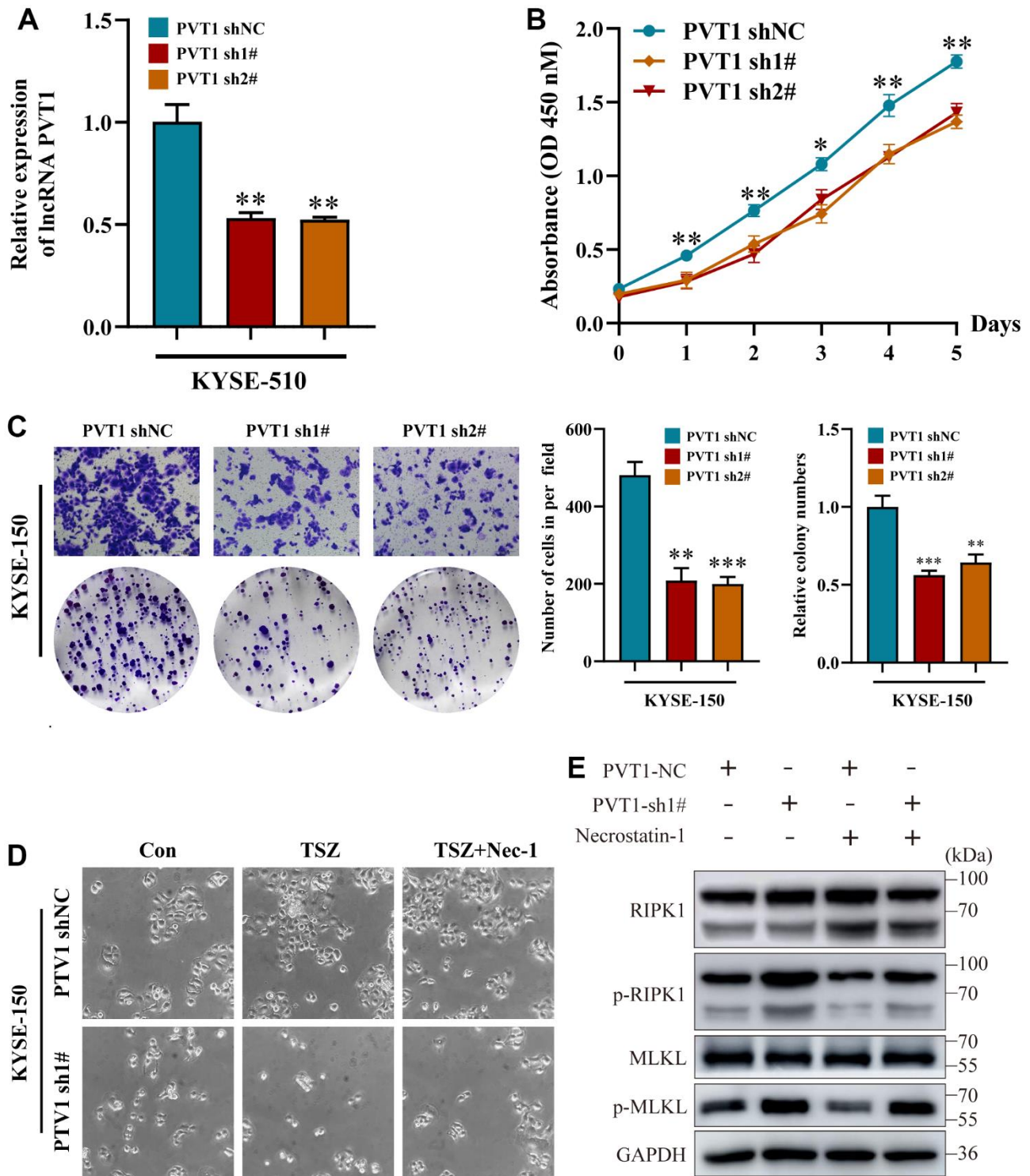
Supplementary Figure 2. Comparison of PCA models based on different gene sets. (A) PCA of all genes. (B) PCA of all necroptosis-related genes. (C) PCA of all co-expressed necroptosis lncRNAs. (D) PCA of six prognostic necroptosis-related lncRNAs.



Supplementary Figure 3. Survival analysis of patients in high- and low-risk groups based on various clinicopathological features. Kaplan–Meier survival curves of (A, B) Age. (C, D) Male. (D, E) Grade. (F) Stage. (G) T. (H, I) N.



Supplementary Figure 4. GSEA enrichment analysis in ESCA patients from distinct risk groups. (A) GSEA enrichment analysis of ESCA patients in the high-risk group. (B) GSEA enrichment analysis of ESCA patients in the low-risk group.



Supplementary Figure 5. PVT1 promoted KYSE-150 cell proliferation, migration, and inhibited necroptosis *in vitro*.

(A) The transfection efficiency of PVT1 was downregulated using shRNAs. (B, C) Knockdown of PVT1 inhibited KYSE-150 cell proliferation and colony formation ability. (D) Both control and KYSE-150 PVT1-sh cells were treated with Nec-1 (50 μ M) for 4 h and then treated with TSZ. After 24 h of drug treatment, the morphological changes of treated cells were imaged under a phase-contrast microscope. (E) Western Blot was performed to detect RIP1, p-RIP1, MLKL, and p-MLKL protein levels. Data are presented as mean \pm SD (* p < 0.05; ** p < 0.01; *** p < 0.001).